Towards better understanding of photophysics of platinum(II) coordination compounds with anthracene and pyrene substituted 2,6-bis(thiazol-2-yl)pyridines

Anna Maria Maroń, Katarzyna Choroba, Tomasz Pedzinski, Barbara Machura

Electronic Supplementary Information

ABSORPTION AND EMISSION SPECTRA IN DICHLOROMETHANE (RT)

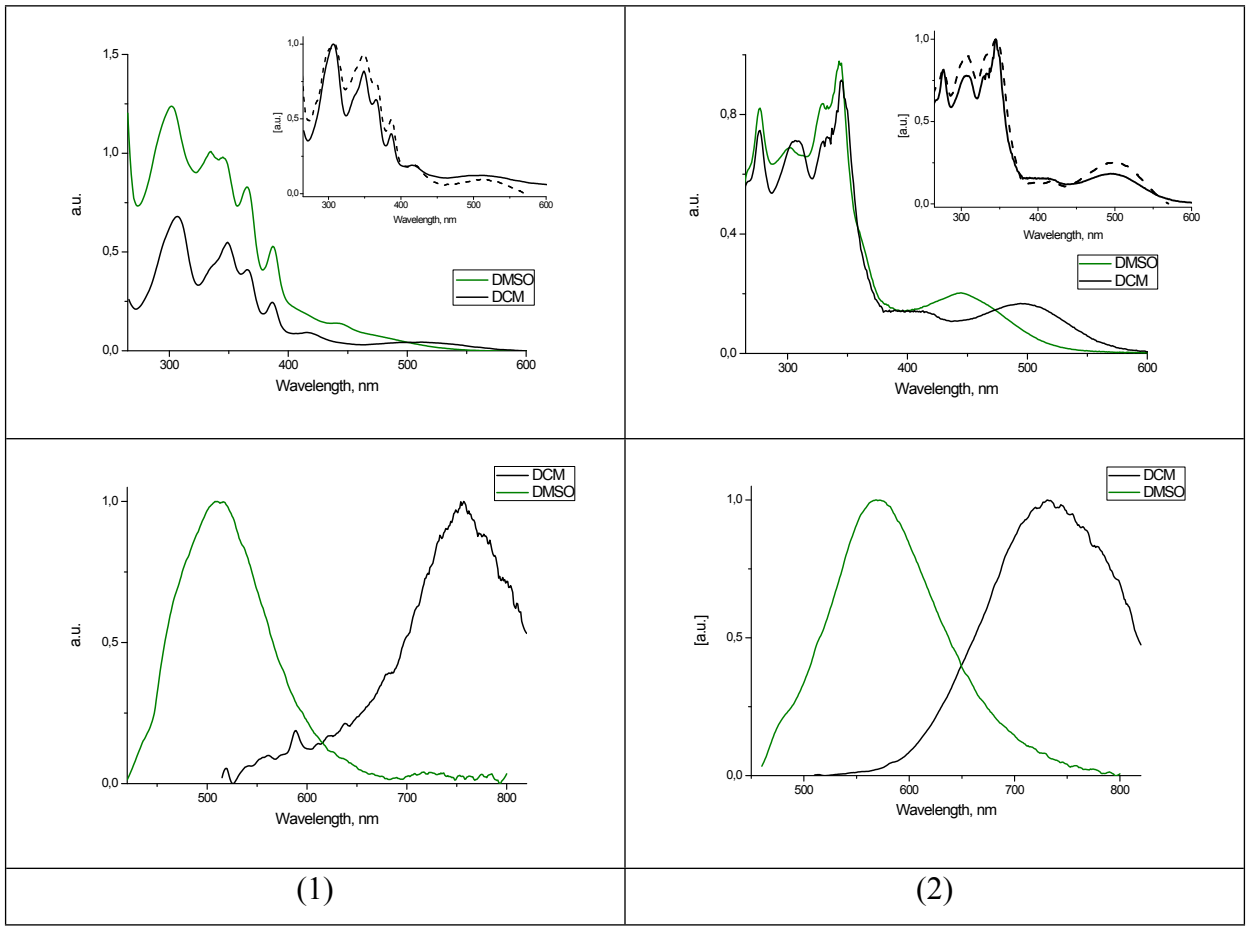

Figure S1. Absorption (upper) and emission (lower) spectra of (**1**) and (**2**) in CH_2Cl_2 with comparison to DMSO solutions[1]. Insert plots: Comparison of normalized absorption (solid) and excitation (dash) spectra of (**1**) and (**2**) in CH_2Cl_2.

Table S1. Photoluminescence properties of (**1**) – (**2**) in CH_2Cl_2

	λ_{exc} [nm]	λ_{em} [nm]	ΔE_{exc-em} [cm^{-1}]	τ [μs] (% weight)	χ^2
(1)	513, 417, 386, 366, 349, 308	755	6248	10.53 (78.88%), 3.8 (21.12%)	1.009
(2)	500, 417, 346, 306, 277	733	6357	11.3 (68.44%), 4.2 (31.56%)	0.982

Scheme S1. Schematic representation of possible deactivation pathways in bichromophoric transition metal compounds possessing ^{3}IL/^{3}ILCT excited state as LEES proposed in Ref [2]: A) efficient ^{1}IL/^{1}ILCT to ^{1}MLCT energy transfer and ^{3}IL/^{3}ILCT and ^{3}MLCT excited states equilibrium; B) efficient and rapid internal conversion/intersystem crossing within the organic ligand subunit; C) inefficient singlet energy transfer to the transition metal chromophore and no ^{3}IL/^{3}ILCT – ^{3}MLCT.

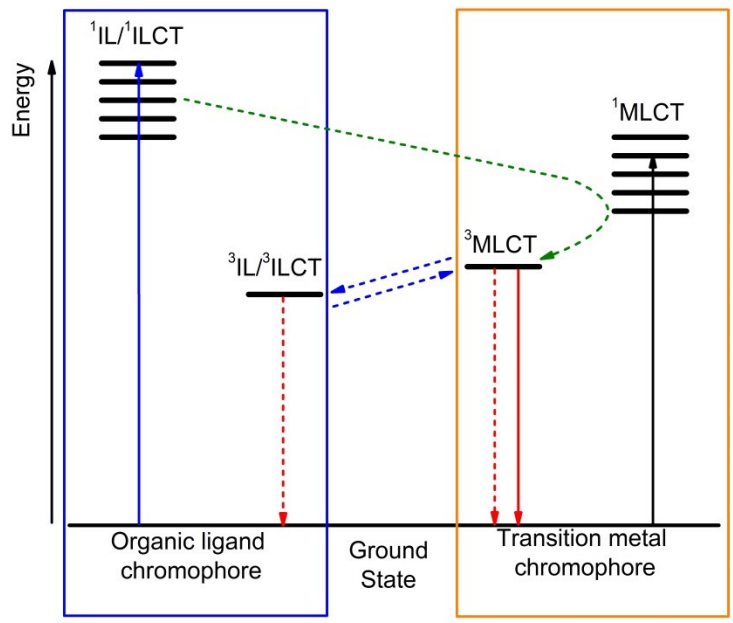

A

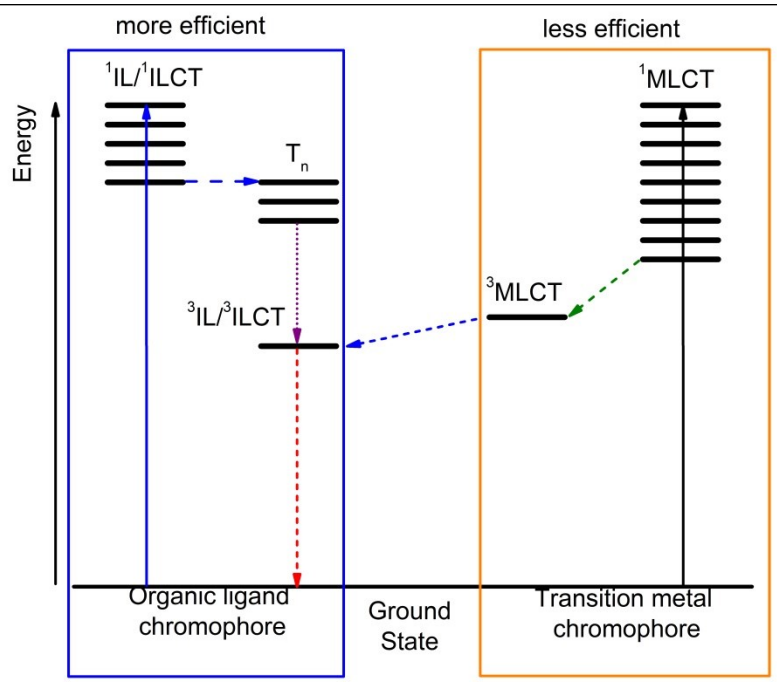
more efficient
less efficient
Energy
^{1}IL/^{1}ILCT
T_n
^{3}IL/^{3}ILCT
^{1}MLCT
^{3}MLCT
Organic ligand chromophore
Ground State
Transition metal chromophore

B

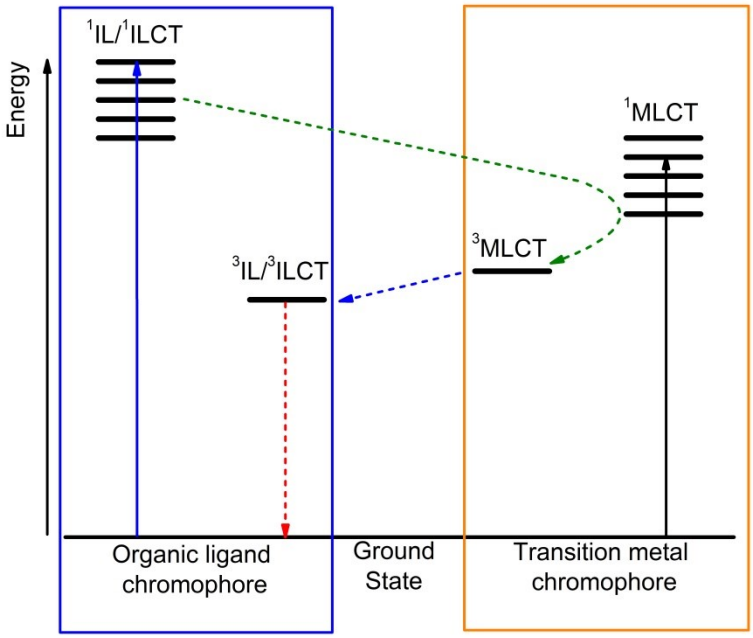
Energy
^{1}IL/^{1}ILCT
^{3}IL/^{3}ILCT
^{1}MLCT
^{3}MLCT
Organic ligand chromophore
Ground State
Transition metal chromophore

C

SINGLET OXYGEN SENSITIZATION

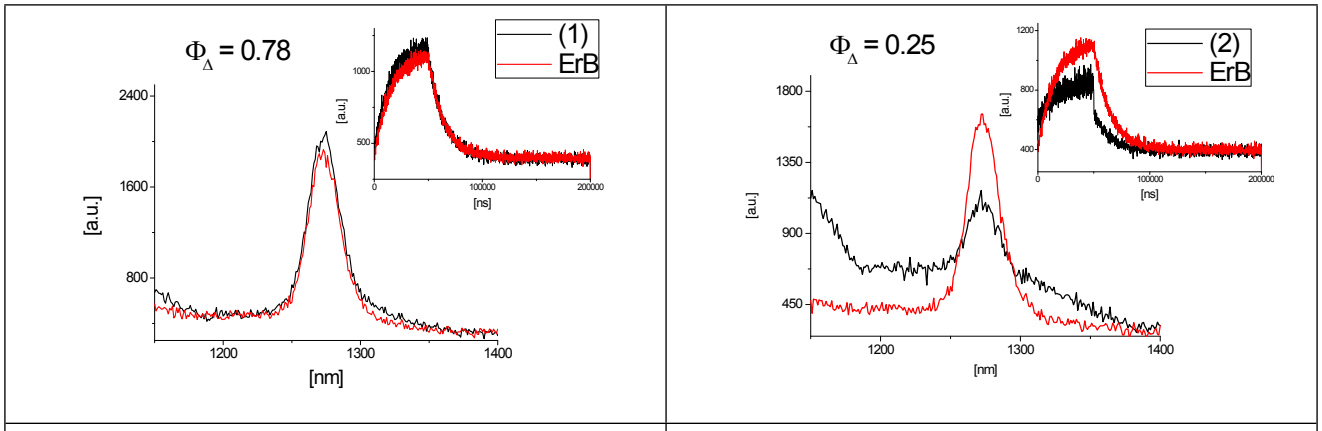

(1)	(2)

Figure S2. Emission peaks of singlet oxygen photogenerated by complexes (**1**)–(**2**) and reference erythrosine B (ErB) (λ_{PE} = 440 nm); Insert plots: decay curves of singlet oxygen phosphorescence generated by (**1**)–(**2**) in relation to ErB in EtOH.

EMISSION PROPERTIES AT 77K

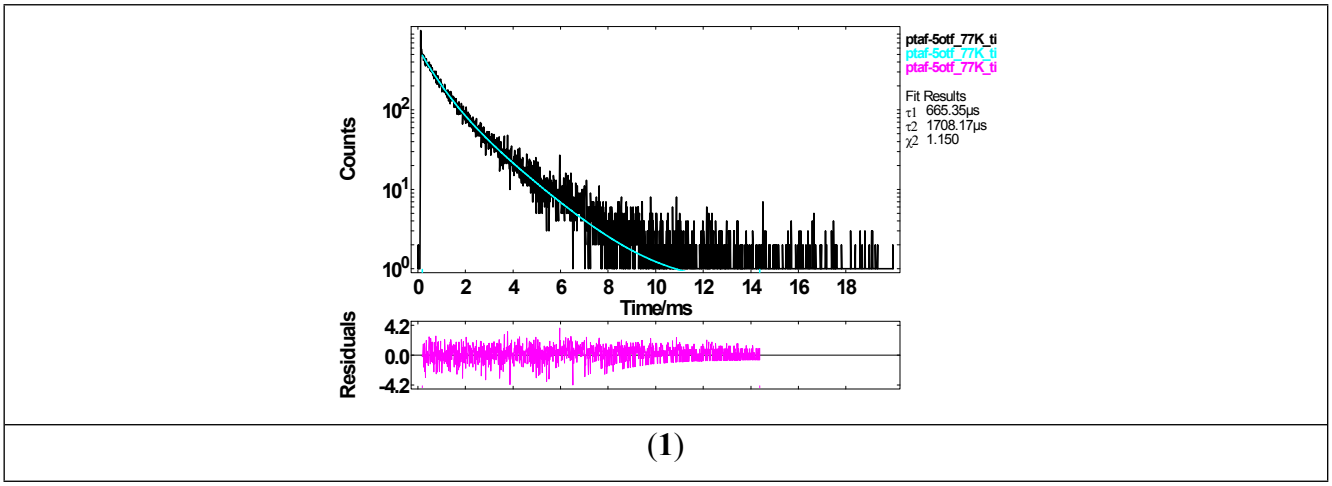

(**1**)

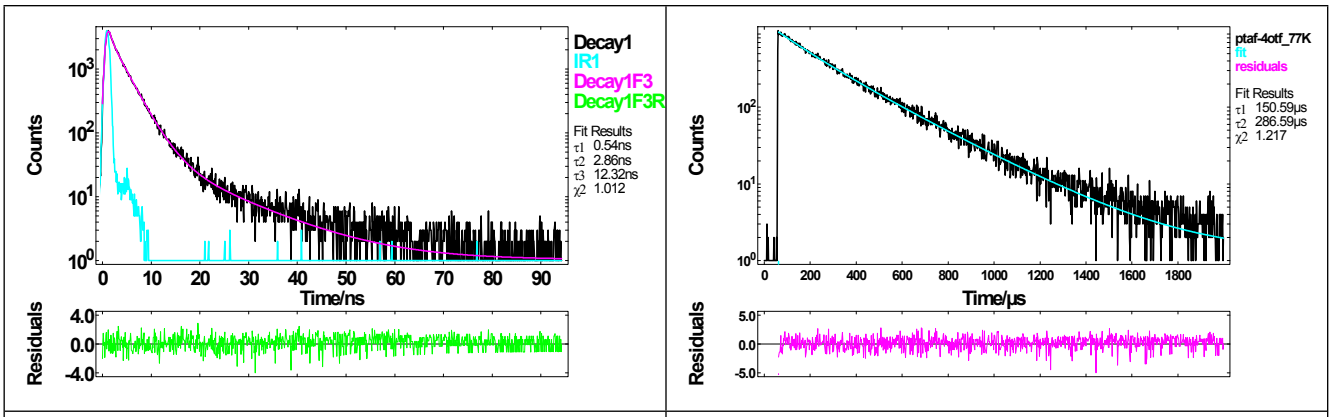

λ_{PL} = 480 nm	λ_{PL} = 660 nm
(**2**)	

Figure S3. Decay curves of 77 K emission of complexes (**1**)–(**2**).

NANOSECOND TRANSIENT ABSORPTION

	(1)	L^1
A	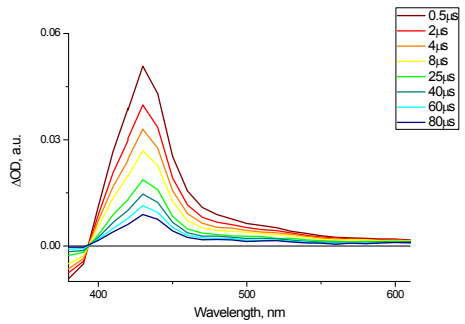	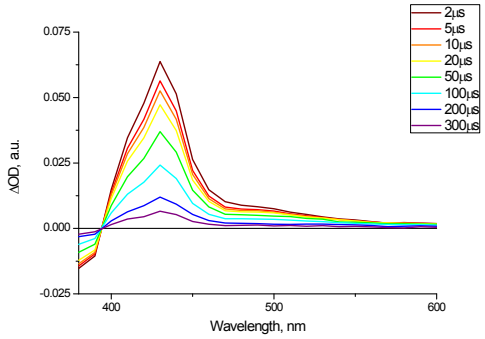
B	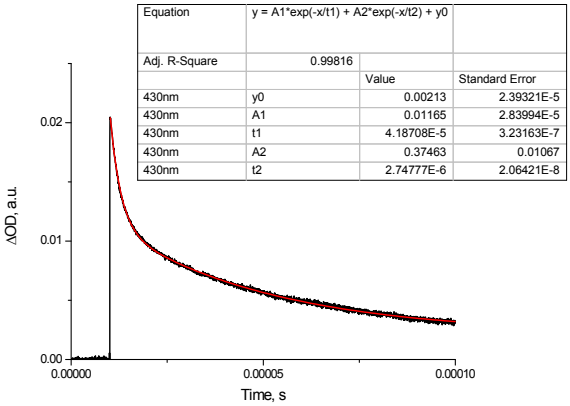 Equation: y = A1*exp(-x/t1) + A2*exp(-x/t2) + y0 Adj. R-Square: 0.99816 Value / Standard Error 430nm y0 0.00213 2.39321E-5 430nm A1 0.01165 2.83994E-5 430nm t1 4.18708E-5 3.23163E-7 430nm A2 0.37463 0.01067 430nm t2 2.74777E-6 2.06421E-8	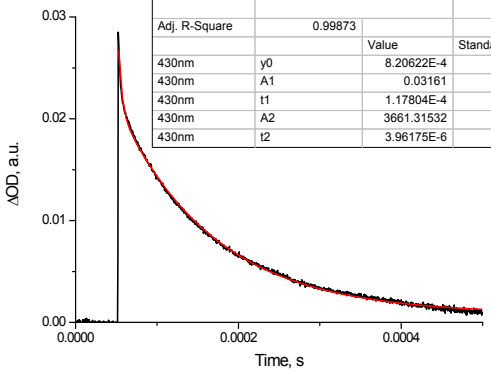 Equation: y = A1*exp(-x/t1) + A2*exp(-x/t2) + y0 Adj. R-Square: 0.99873 Value / Standard Error 430nm y0 8.20622E-4 1.82198E-5 430nm A1 0.03161 9.19089E-5 430nm t1 1.17804E-4 4.6458E-7 430nm A2 3661.31532 1882.14603 430nm t2 3.96175E-6 1.49116E-7
	τ_1: 41.87µs, τ_2: 2.75µs (Ar)	**τ_1: 117.80µs τ_2: 3.96µs (Ar)**
C	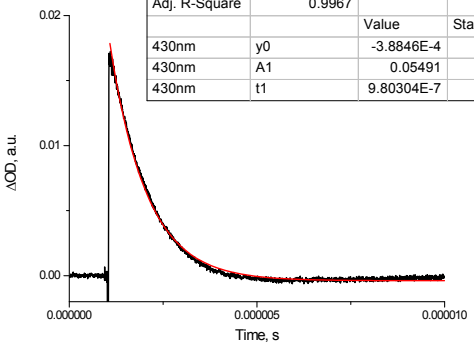 Equation: y = A1*exp(-x/t1) + y0 Adj. R-Square: 0.9967 Value / Standard Error 430nm y0 -3.8846E-4 6.15507E-6 430nm A1 0.05491 2.1399E-4 430nm t1 9.80304E-7 2.48697E-9	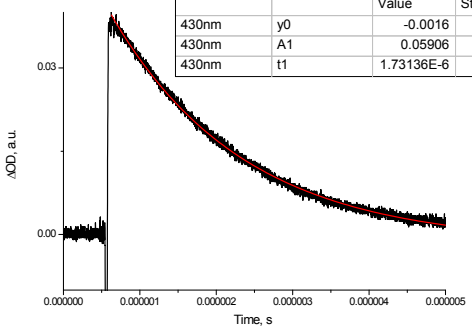 Equation: y = A1*exp(-x/t1) + y0 Adj. R-Square: 0.99728 Value / Standard Error 430nm y0 -0.0016 4.05896E-5 430nm A1 0.05906 6.01451E-5 430nm t1 1.73136E-6 4.81361E-9
	τ_1: 0.98µs (Air)	**τ_1: 1.73µs (Air)**

Figure S4. Nanosecond transient absorption spectra (A) and kinetic fit at λ = 430 nm of argon bubbled (B) and air-equilibrated (C) DMSO solutions of (**1**) and **L^1**

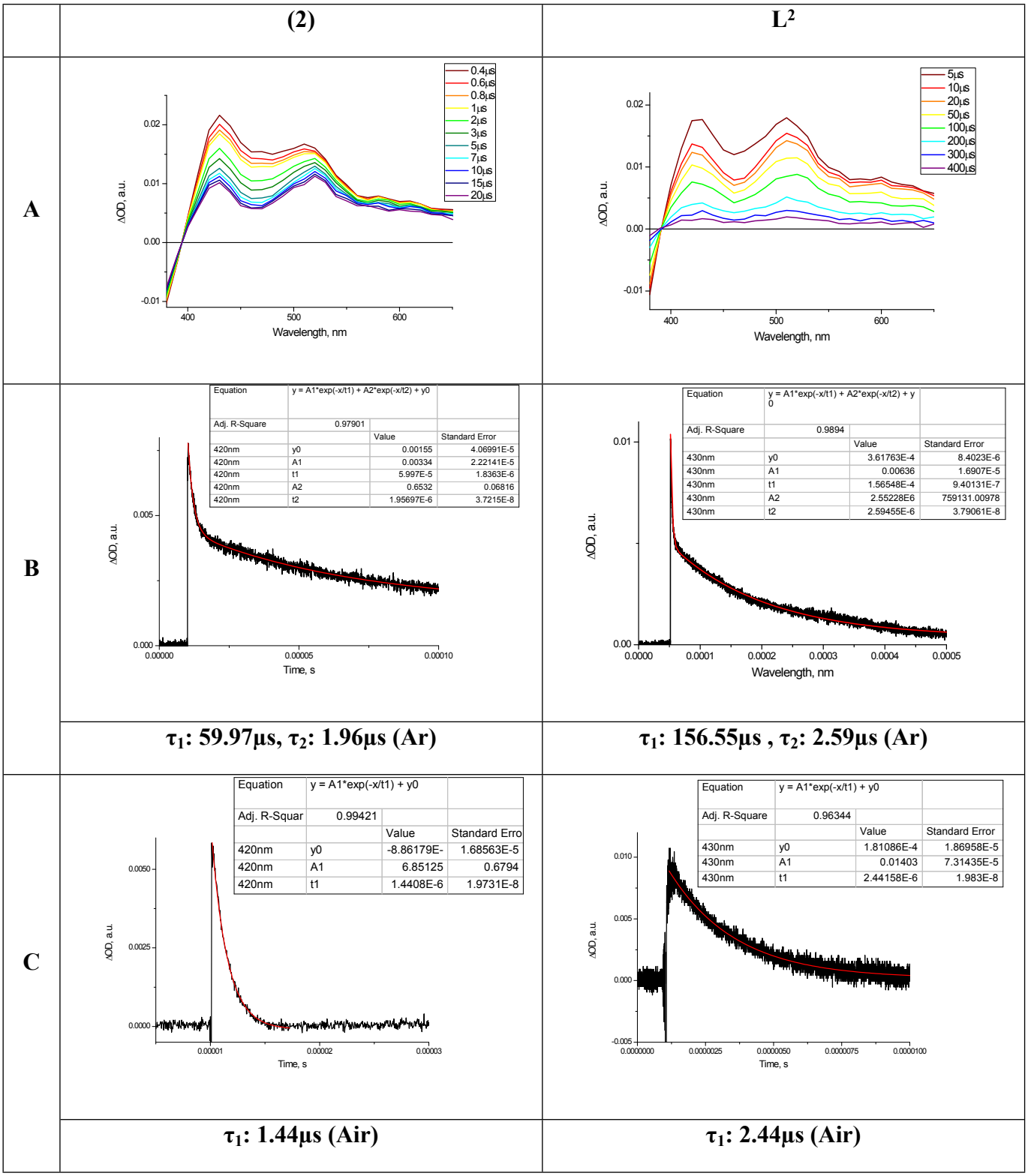

Figure S5. Nanosecond transient absorption spectra (A) and kinetic fit at λ = 420 nm of argon bubbled (B) and air-equilibrated (C) DMSO solutions of (**2**) and **L²**

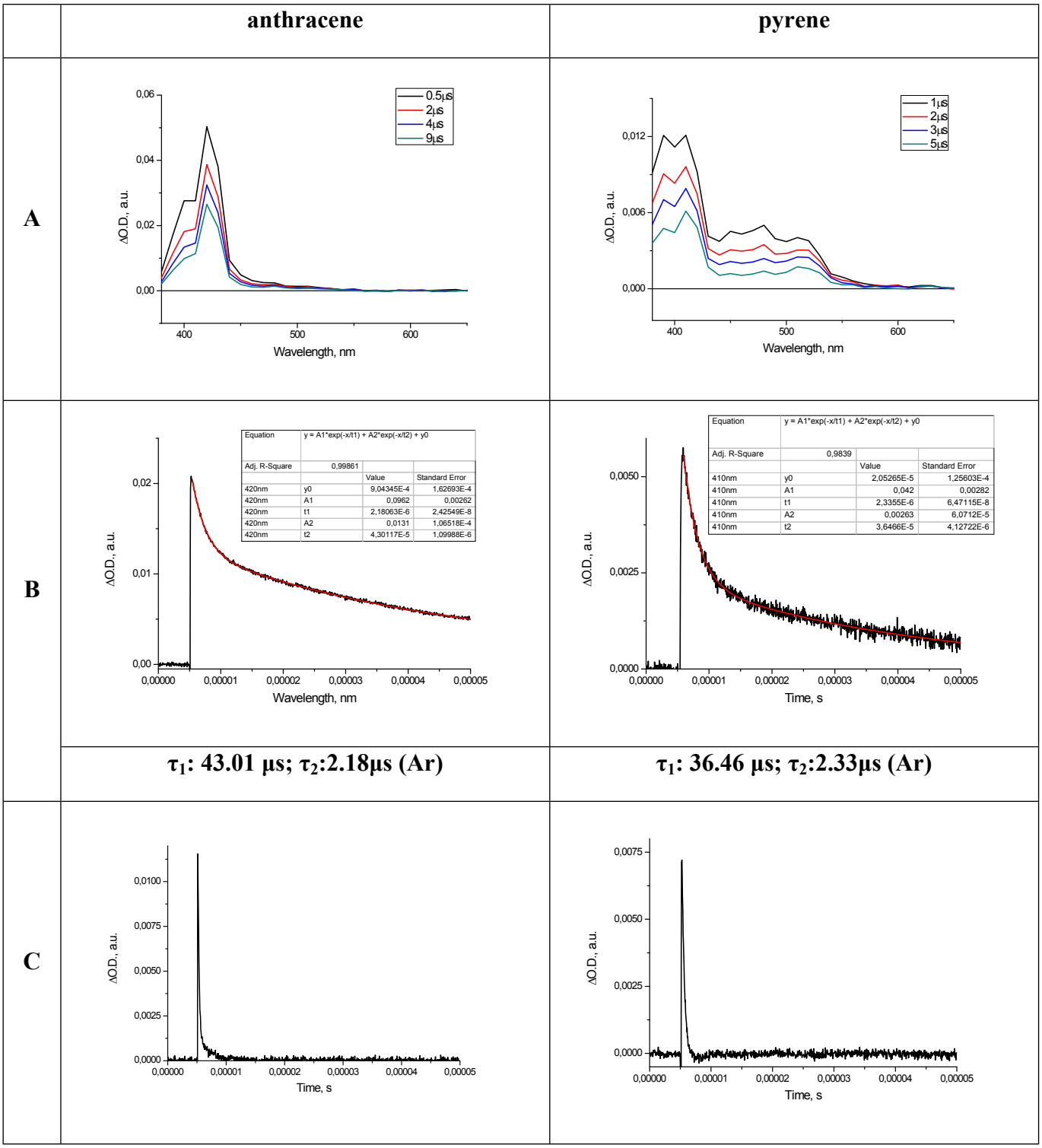

Figure S6. Nanosecond transient absorption spectra (A) and kinetic traces at λ = 420 nm (anthracene)/410nm (pyrene) of argon bubbled (B) and air-equilibrated (C) solutions of anthracene and pyrene.

FEMTOSECOND TRANSIENT ABSORPTION

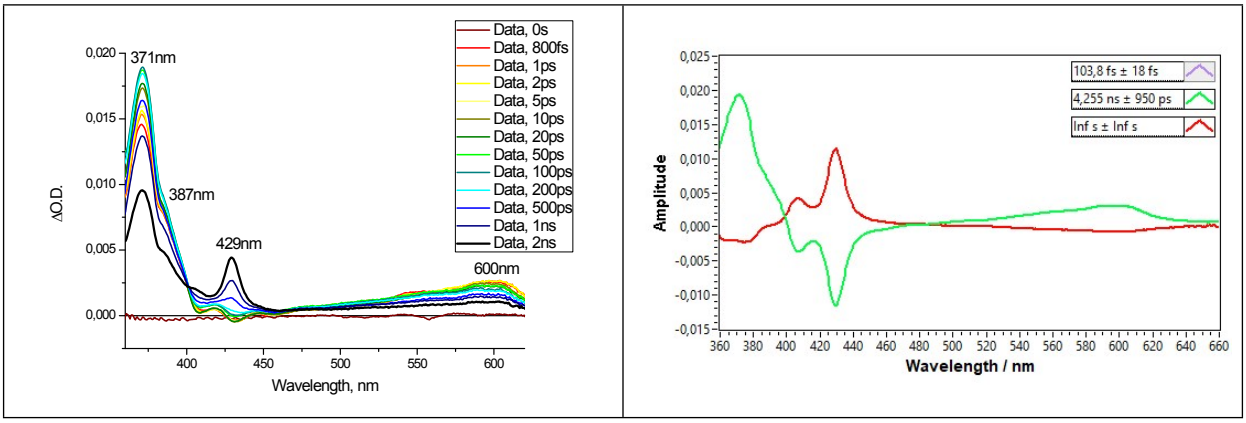

Figure S7. Femtosecond transient absorption spectra and decay associated spectrum of anthracene.

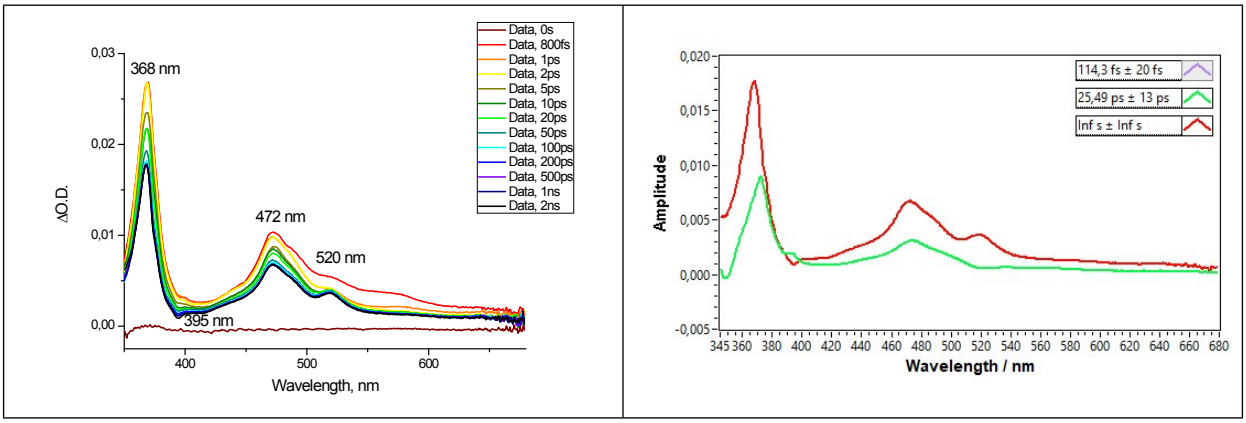

Figure S8. Femtosecond transient absorption spectra and decay associated spectrum of pyrene.

ANALYTICAL DATA FOR L^1, L^2, (1) and (2)

L^1: $C_{25}H_{15}N_3S_2$ (421.54 g mol^{-1}): calcd C 71.25%, H 3.58%, N 9.97%; found C 71.54%, H, 3.66%, N 9.79%.**^{1}H NMR (400 MHz, $CDCl_3$) δ** 8.57 (s, 1H), 8.35 (s, 2H), 8.08 (d, *J* = 8.5 Hz, 2H), 7.92 (d, *J* = 3.0 Hz, 2H), 7.69 (d, *J* = 8.8 Hz, 2H), 7.53 (d, *J* = 3.0 Hz, 2H), 7.51 – 7.46 (m, 2H), 7.42 – 7.36 (m, 2H). **^{13}C NMR (100 MHz, $CDCl_3$) δ** 168.74, 151.57, 150.40, 144.44, 133.00, 131.36, 129.53, 128.71, 128.08, 126.38, 126.03, 125.48, 123.08, 122.13.

L^2: $C_{27}H_{17}N_3S_2$ (447.44 g mol^{-1}): calcd C 72.47%; H 3.83%; N 14.30%; found: C 72.13%; H 3.69%; N 14.47.**^{1}H NMR (400 MHz, $CDCl_3$) δ** 8.54 (s, 2H), 8.30 – 8.20 (m, 4H), 8.16 – 8.03 (m, 5H), 7.97 (d, *J* = 3.1 Hz, 2H), 7.54 (d, *J* = 3.1 Hz, 2H). **^{13}C NMR (100 MHz, $CDCl_3$) δ** 168.88, 152.02, 151.33, 144.38, 133.88, 131.85, 131.52, 130.99, 128.77, 128.39, 128.37, 127.49, 127.26, 126.42, 125.82, 125.55, 125.06, 124.97, 124.86, 124.27, 122.13, 122.01.

(1): $C_{25}H_{15}S_2N_3ClPt$, CF_3SO_3: calcd C 38.98%, H 1.89%, N 5.25%; found: C 38.73%; H 1.884%; N 5.537%. **IR (KBr; cm^{-1}):** 3437$\nu_{(OH)}$, 3124, 3066$\nu_{(ArH)}$; 1607 $\nu_{(C=N,\ C=C)}$; 1451 $\delta_{(C–CH\ out\ of\ the\ plane)}$; 1255 $\nu_{a(SO3)}$, 1153$\nu_{(C–N)}$; 1092 $\delta_{(C–CH\ in\ the\ plane)}$; 1030 $\nu_{s(SO3)}$; 895 $\delta_{(C–C\ out\ of\ the\ plane)}$, 732 $\delta_{(C–C\ out\ of\ the\ plane)}$; 634 $\delta_{(SO3)}$. **^{1}H NMR (400 MHz, ppm)** δ 8.90 (s, 1H, H^{C8}), 8.88 (s, 2H, H^{B2}), 8.48 (d, *J* = 3.4 Hz, 2H, H^{A1}), 8.27 (d, *J* = 8.4 Hz, 2H, H^{C3}), 8.03 (d, *J* = 3.4 Hz, 2H, H^{A2}), 7.87 (d, *J* = 8.7 Hz, 2H, H^{C6}), 7.66 – 7.55 (m, 4H, $H^{C4,\ C5}$). **^{13}C NMR (100 MHz, ppm) δ** 169.71 (C^{A3}), 153.87 (C^{C1}), 151.07 (C^{B1}), 140.88 (C^{A2}), 130.98 (C^{C2}), 130.65 (C^{C7}), 129.00 (C^{A1}), 128.79 (C^{C3}), 128.67 (C^{C8}), 127.05 ($C^{C4,\ C5}$), 126.09 ($C^{C4,\ C5}$), 125.82 (C^{B2}), 125.60 (C^{C6}).

(2): $C_{27}H_{15}S_2N_3ClPt$, CF_3SO_3: calcd C 40.76%, H 1.83%, N 5.09%; found: C 40.54%, H 1.904%, N 4.943%. **IR (KBr; cm^{-1}):** 3454 $\nu_{(OH)}$, 3067, 2922 $\nu_{(ArH)}$; 1606 $\nu_{(C=N,\ C=C)}$; 1483, 1453 $\delta_{(C–CH\ out\ of\ the\ plane)}$; 1253, 1152$\nu_{(C–N)}$; 1079 $\delta_{(C–CH\ in\ the\ plane)}$; 1028 $\nu_{s(SO3)}$; 849 $\delta_{(C–C\ out\ of\ the\ plane)}$, 721 $\delta_{(C–C\ in\ the\ plane)}$; 636 $\delta_{(SO3)}$. **^{1}H NMR (400 MHz, ppm) δ** 8.88 (s, 2H, H^{B2}), 8.48 – 8.45 (m, 3H, H^{A1+C13}), 8.41 (d, *J* = 7.6 Hz, 1H, H^{C8}), 8.34 – 8.30 (m, 4H, $H^{C10+C6+C3+C2}$), 8.27 – 8.23 (m, 2H, H^{C12+C5}), 8.14 (t, *J* = 7.6 Hz, 1H, H^{C9}), 7.93 (d, *J* = 3.4 Hz, 2H, H^{A2}). **^{13}C NMR (100 MHz, ppm) δ** 169.01 (C^{A3}), 154.57 (C^{C1}), 150.10 (C^{B1}), 140.70 (C^{A2}), 131.96 (C^{C4}), 131.50 (C^{C7}), 130.79 (C^{B3}), 130.15 (C^{C2}), 129.16 (C^{A1}), 129.08 (C^{C6}), 128.86 (C^{C11}), 127.51 (C^{C9}), 127.46 (C^{C12}), 127.15 (C^{C5}), 126.89 (C^{C14}), 126.52 (C^{C8}), 125.79 (C^{C13}), 125.05 (C^{C10}), 124.78 (C^{B2}), 123.83 (C^{C3}), 123.62 ($C^{C15,\ C16}$), 123.51 ($C^{C15,\ C16}$).

STABILITY STUDIES IN DMSO SOLUTIONS

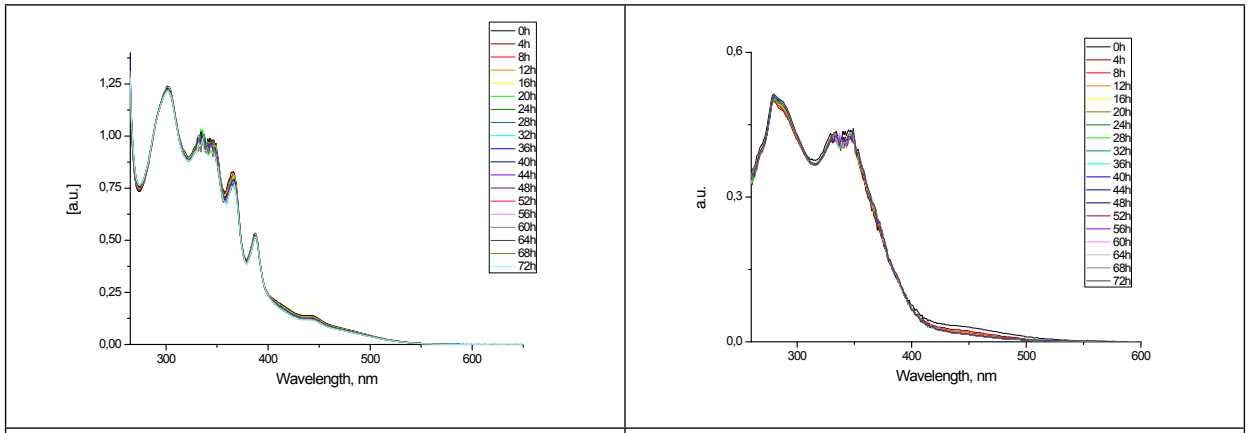

(**1**)	(**2**)

Figure S9. Stability studies in DMSO solution of compounds (**1**) and (**2**).

REFERENCES

[1] K. Choroba, B. Machura, L. R Raposo, J. G. Małecki, S. Kula, M. Pająk, K. Erfurt, A. Maroń, A. R Fernandes, *Dalton Transactions*, 2019, **48**, 13081−13093

[2] J. E. Yarnell, K. A. Wells, J. R. Palmer, J. M. Breaux, F. N. Castellano, *J. Phys. Chem. B* 2019, **123**, 7611−7627